GSA Data Repository 2018007
A geologic recipe for transient slip within the seismogenic zone: insight from the Guerrero seismic gap
Husker, Ferrari, Arango-Galván, Corbo-Camargo, Arzate-Flores

MT Resolution

MT resolution can be understood both qualitatively and quantitatively. Qualitatively, resolution deteriorates with depth and conductivity. A highly conductive body near the surface will be imaged well, but another conductive body below that will be harder to image. This can be seen in the differences between P1 and P3 or P4 (Fig. 2). Both P3 and P4 show a crisp image of a shallow conductive body. However, the deeper conductive body in P1 has a well-defined roof, but the floor is diffuse with no clear bottom. Moreover, the shallow conductive body (> 30 km from the coast) in P1 has a well-defined roof and floor, but the possible extension (> 30 km from the coast) of the deeper conductive body disappears beneath the more conductive part of the shallow body.

Quantitatively the model resolution was verified by a standard procedure in which a modification is imposed on the model and then it is inverted again to determine if the rest of the model can accommodate imposed constraint. If the difference between the model and the observed data (measured as the rms misfit) does not increase due to the constraint, the model is non-unique (e.g. Saltzer and Humphreys, 1997; Allen and Tromp, 2005). This was done with around 30 different imposed constraints to confirm that the misfit is lowest with the presented model.

Station spacing density was limited by the topography and security issues. The terrain quickly moves from the coast to the mountains. As such it is difficult to find many open flat and level areas, particularly further inland where it is the beginning of the Sierra Madre. The measurement within the Gap (P1) was limited to just 50 km from the coast because further inland in the high Sierra, the territory is controlled by drug traffickers. Thus, we limited all profiles to the same distance. Nonetheless, various studies in Mexico have similar, but varying sounding spacing (3 – 7 soundings within 50 km from the coast) and different MT equipment but all coincide that high conductivity outside of the Gap is within the crust (Jodicke et al., 2006; Corbo-Camargo et al., 2013; Arzate-Flores et al., 2016). Jodicke et al. (2006) published the P2 results and an MT profile that was in the same location as P4 (DR3). The Jodicke et al. (2006) MT profile at P4 had lower resolution than Arzate-Flores et al. (2016) due to using older equipment, but both showed the same basic feature of high conductivity in the crust.

The spatial resolution and the maximum depth that the technique provides is largely due to the frequency range/sampling rate used by the equipment. The observation of shallow and deep conductivity is well within these ranges of the equipment. The only complicated formation is in the part of the Gap further from the coast where there is

high conductivity both deep and shallow with resistivity between the two. This is observed on 2 of the MT soundings which gives us confidence that it is real.

Three different examples of squeeze tests (Allen and Tromp, 2005) are shown in figures DR3- DR14. The three tests are: (1) A conductor on the left side of the figure is and lowered; (2) a large conductor in the middle-left is raised and lowered; and (3) a resistive body on the right is raise and lowered. The tests are each divided into a set of 4 figures, where the first shows the final model, the second the body raised, the third the body lowered, and the forth shows the RMS error with respect to changes in depth of the conductive/resistive bodies for the stations directly above each of the bodies. For example, DR4 shows the effect of raising a conductive body beneath PN05 by 10 km. DR4 can be compared with DR3 to see that the model does not fit as well for DR4 and the RMS error is higher. The RMS with depth (DR6, DR10, DR14) shows that there is a strong minimum in the error at the position our study finds each of the bodies, and deviations of only about 2 km significantly increase the error. All of the images indicate that deviations away from the final MT image do not fit the data as well as the final model. Most importantly, our results show that the conductivity discussed in the paper must be deep and the model does not fit the observations of a shallow conductive body above the slab interface (DR4, DR8). The figure captions explain each squeeze test.

Supplementary Figures

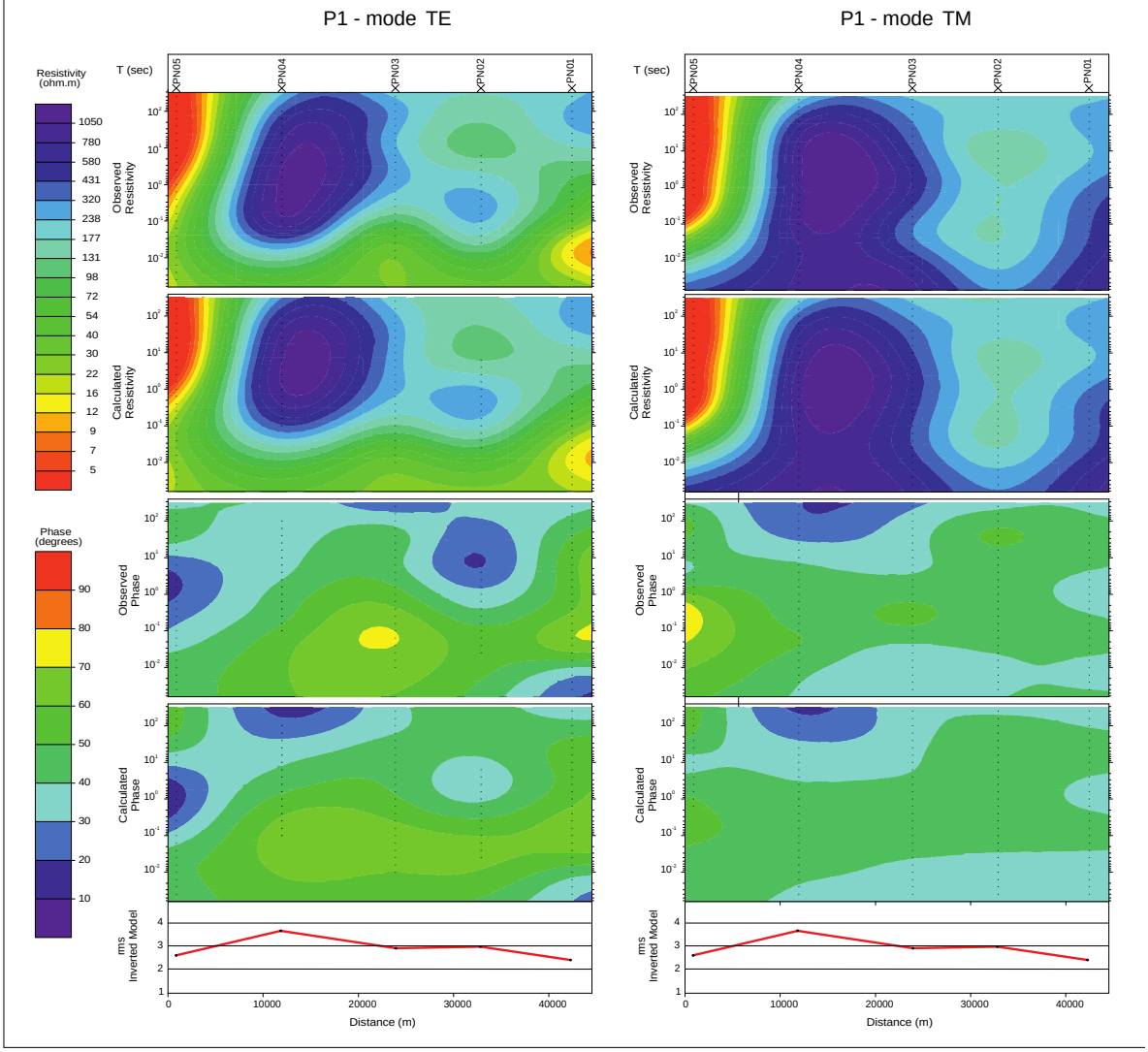

Figure DR1: Observed and calculated apparent resistivity and phase pseudo-sections for P1 (TE and TM modes). The calculated responses from the model matches the observed data across the spectrum of periods (T) well and results in a low rms of less than 4% at all stations.

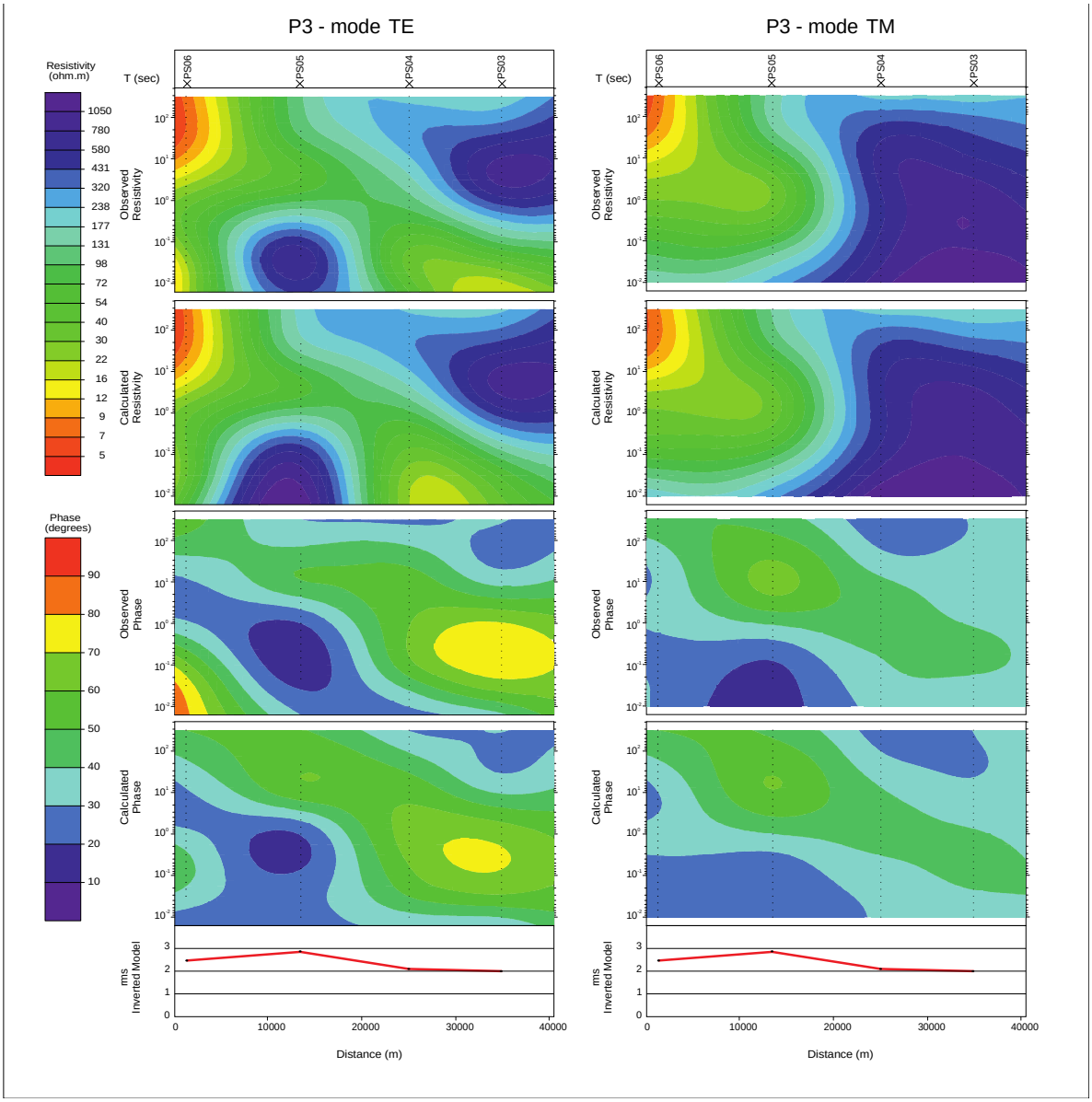

Figure DR2: Observed and calculated apparent resistivity and phase pseudo-sections for P3 (TE and TM modes). The calculated responses from the model matches the observed data across the spectrum of periods (T) well and results in a low rms of less than 4% at all stations.

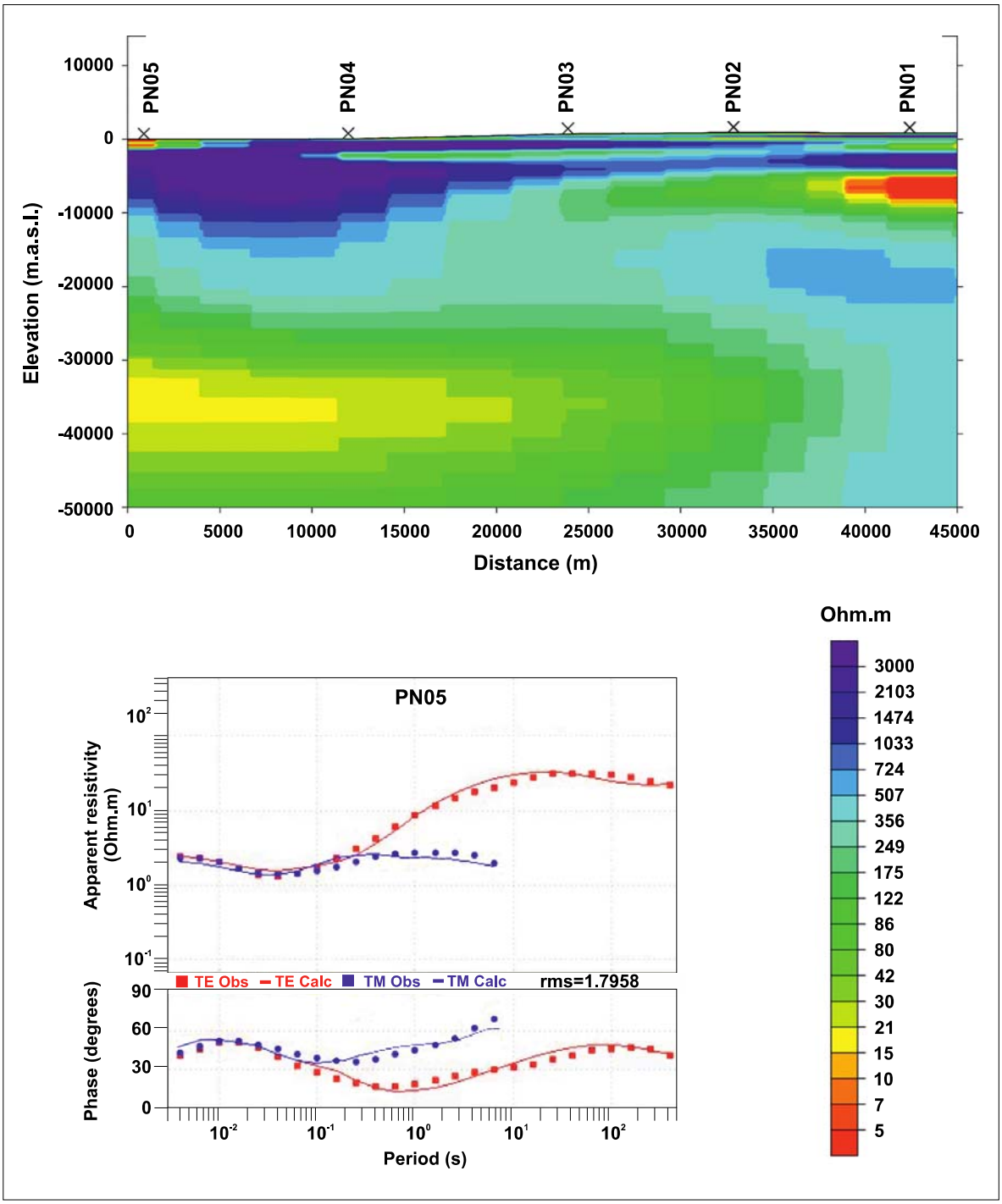

Figure DR3: The top figure shows the final model used in the main text. The bottom figure shows the observations and model at PN05 near the coast. Upper curves display apparent resistivity (Ohm) vs. period (sec). Bottom curves display phases (deg) vs. period (sec). Squares indicate observed curves, and continuous lines indicate model responses. Red color for TE mode and blue color for TM mode. The RMS indicates the error only for this station

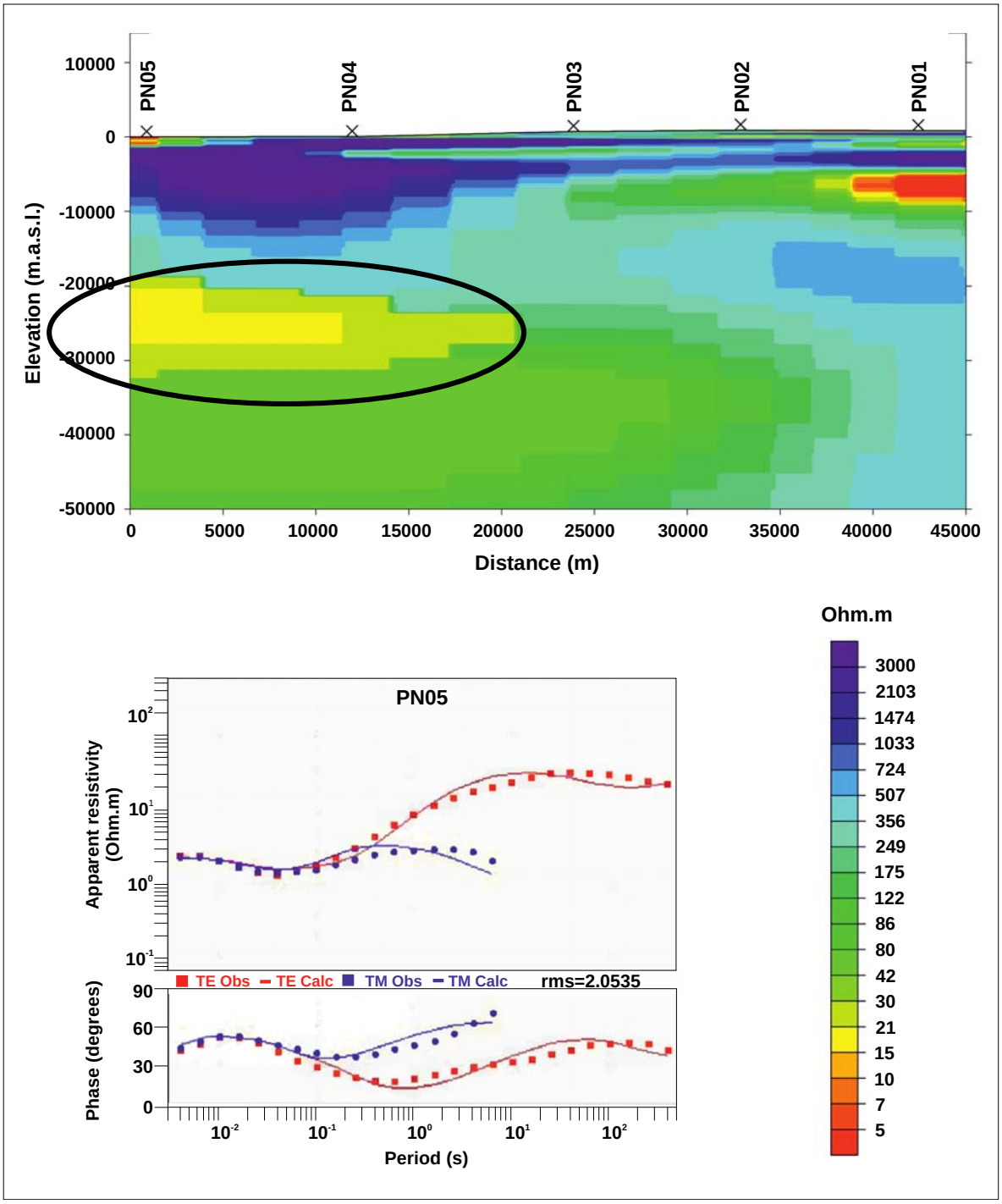

Figure DR4: The top figure shows the squeezing used in this case, which assumes that the top of the conductive body ranging from 15 to 30 Ohms (yellowish colors), located to the south of the profile is 10 km shallower. The bottom figure is explained in DR3.

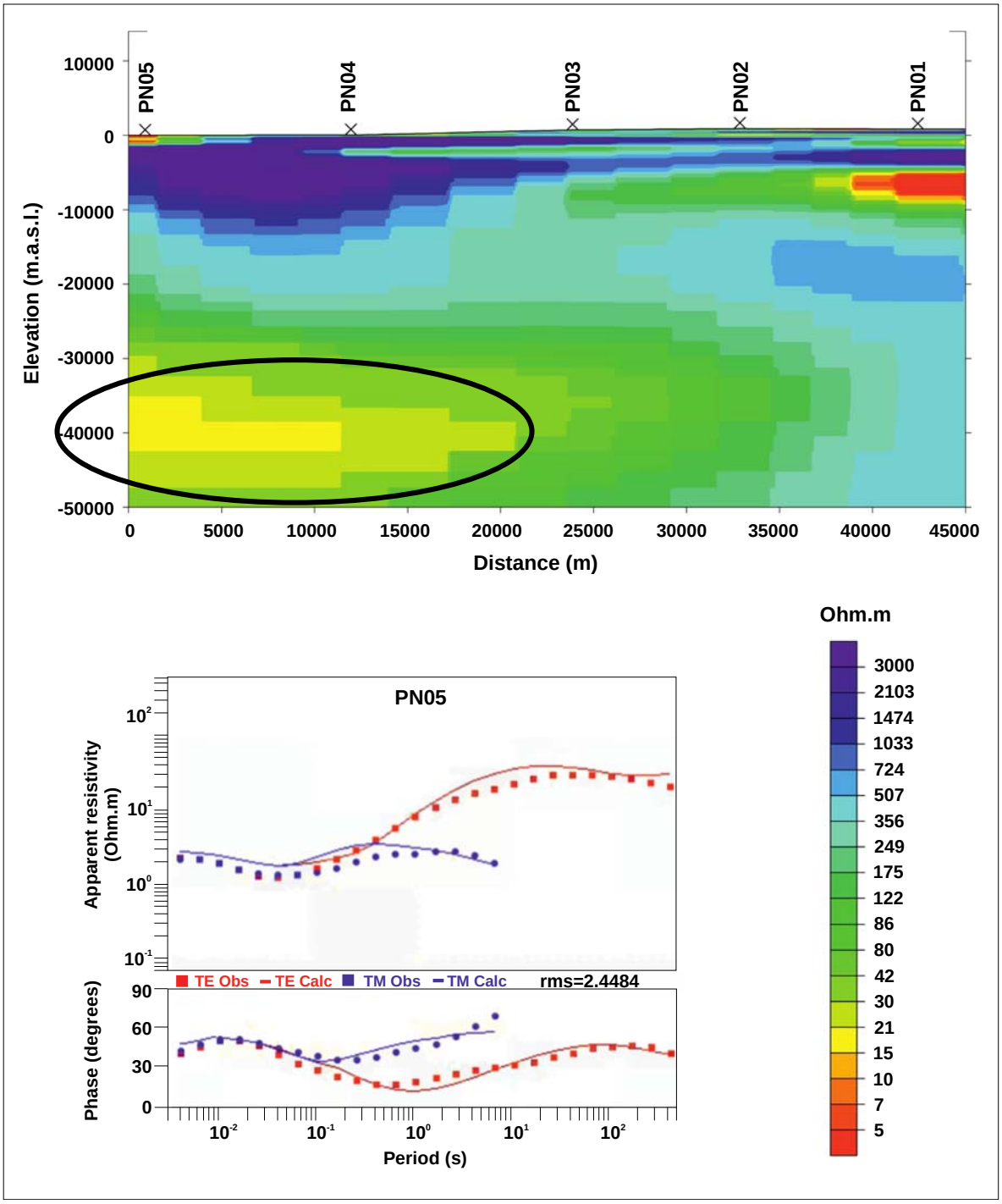

Figure DR5: The top figure shows the squeezing used in this case, which assumes that the same conductive body adjusted in DR4 is 10 km deeper. The bottom figure is explained in DR3.

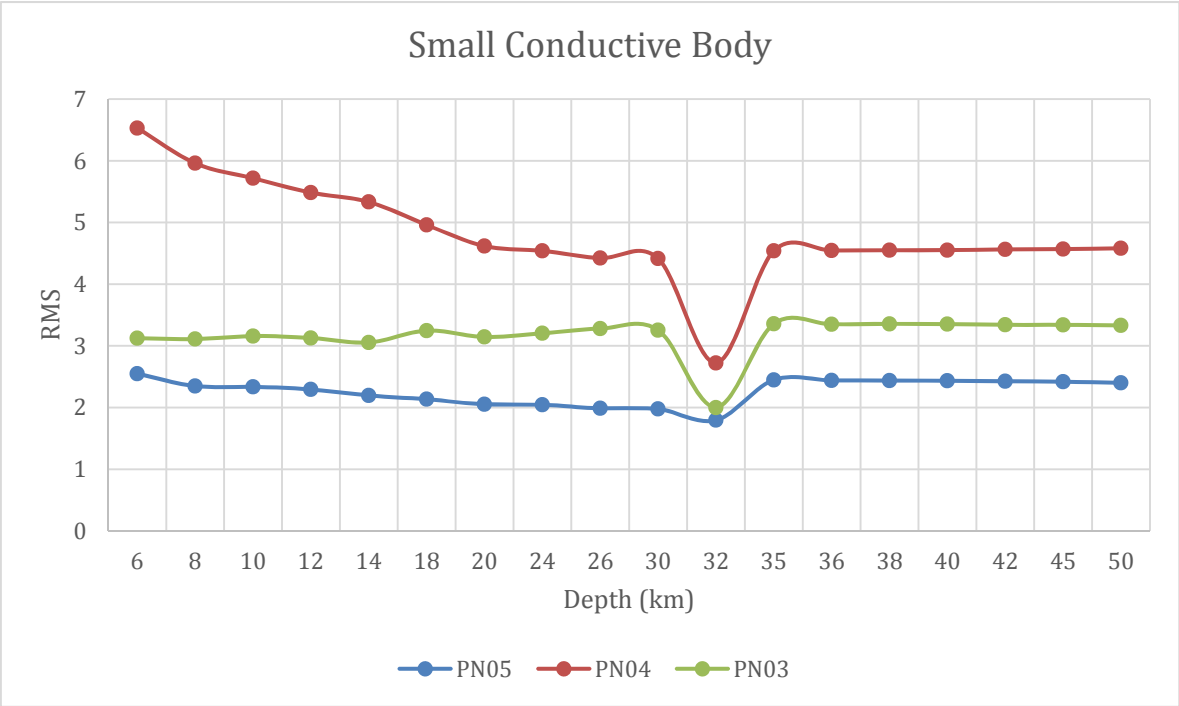

Figure DR6: This figure shows the RMS error from moving the conductive body in DR3 - DR5 steps of 2 km depths for stations PN05, PN04 and PN03 which are located above the body. PN05 is less sensitive to changes in depth due to it being located very close to the ocean, a large conductor. However, PN04 and PN03, which are further inland, clearly show a strong minimum at the depth where our model finds the conductive body.

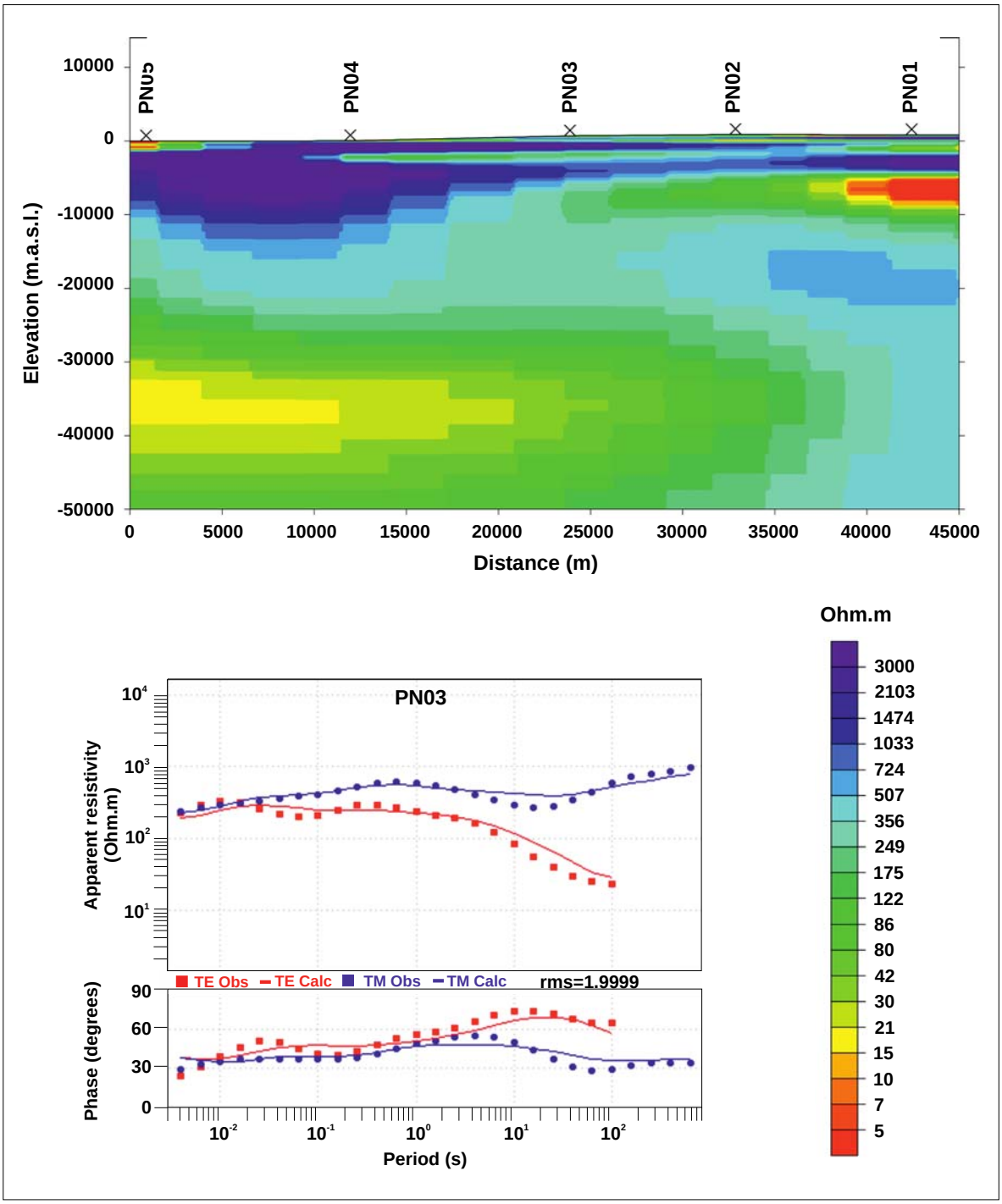

Figure DR7: The top figure shows the final model used in the main text. The bottom figure is explained in DR3, but is for sounding PN03 in the middle of the profile instead of PN05.

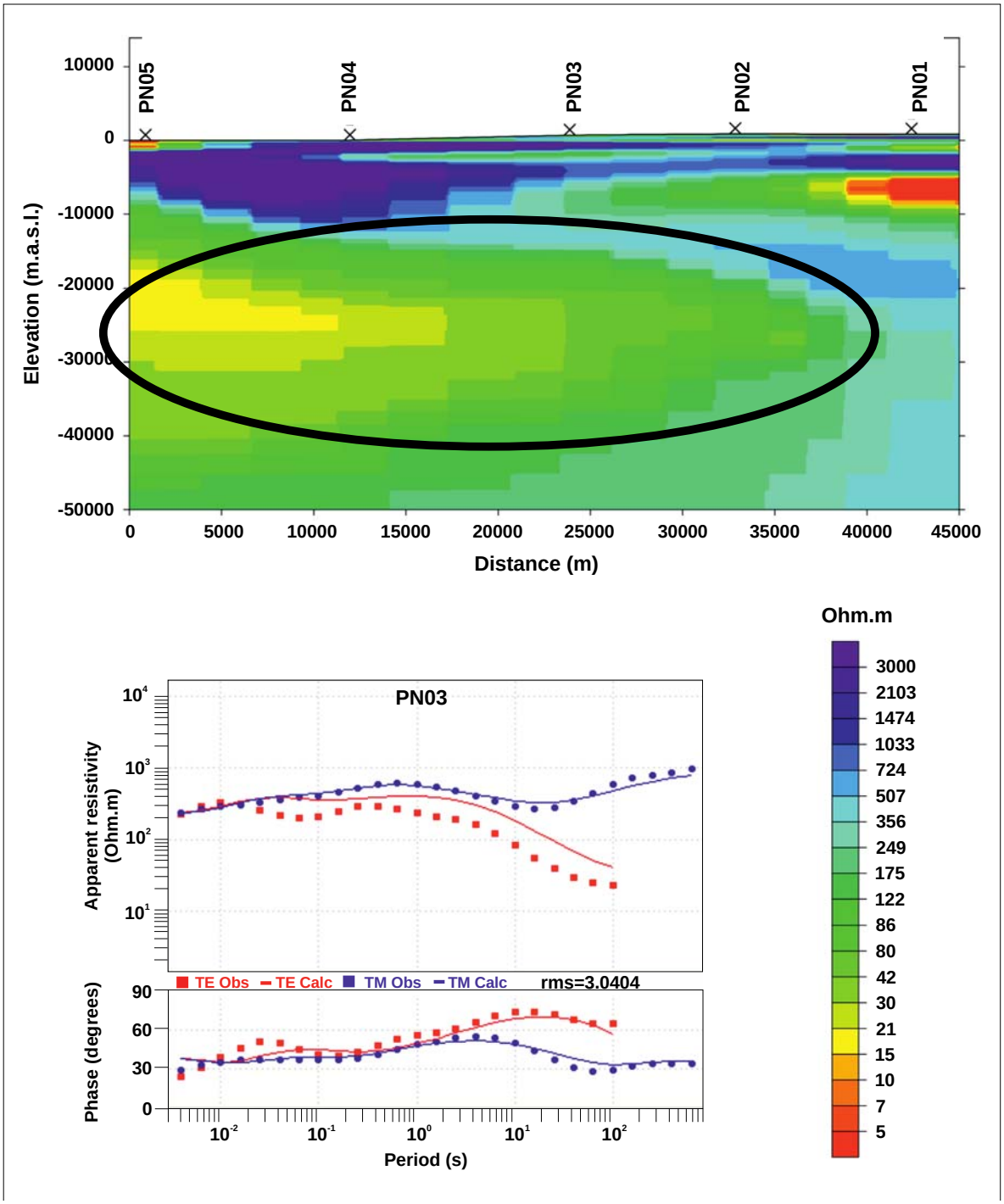

Figure DR8: The top figure shows the squeezing used in this case, which is that the top of the medium conductive body ranging from 30 to 122 Ohms (yellow-greenish colors), located to the middle of the profile is shallower. The bottom figure is explained in DR3, but uses PN03 instead of PN05.

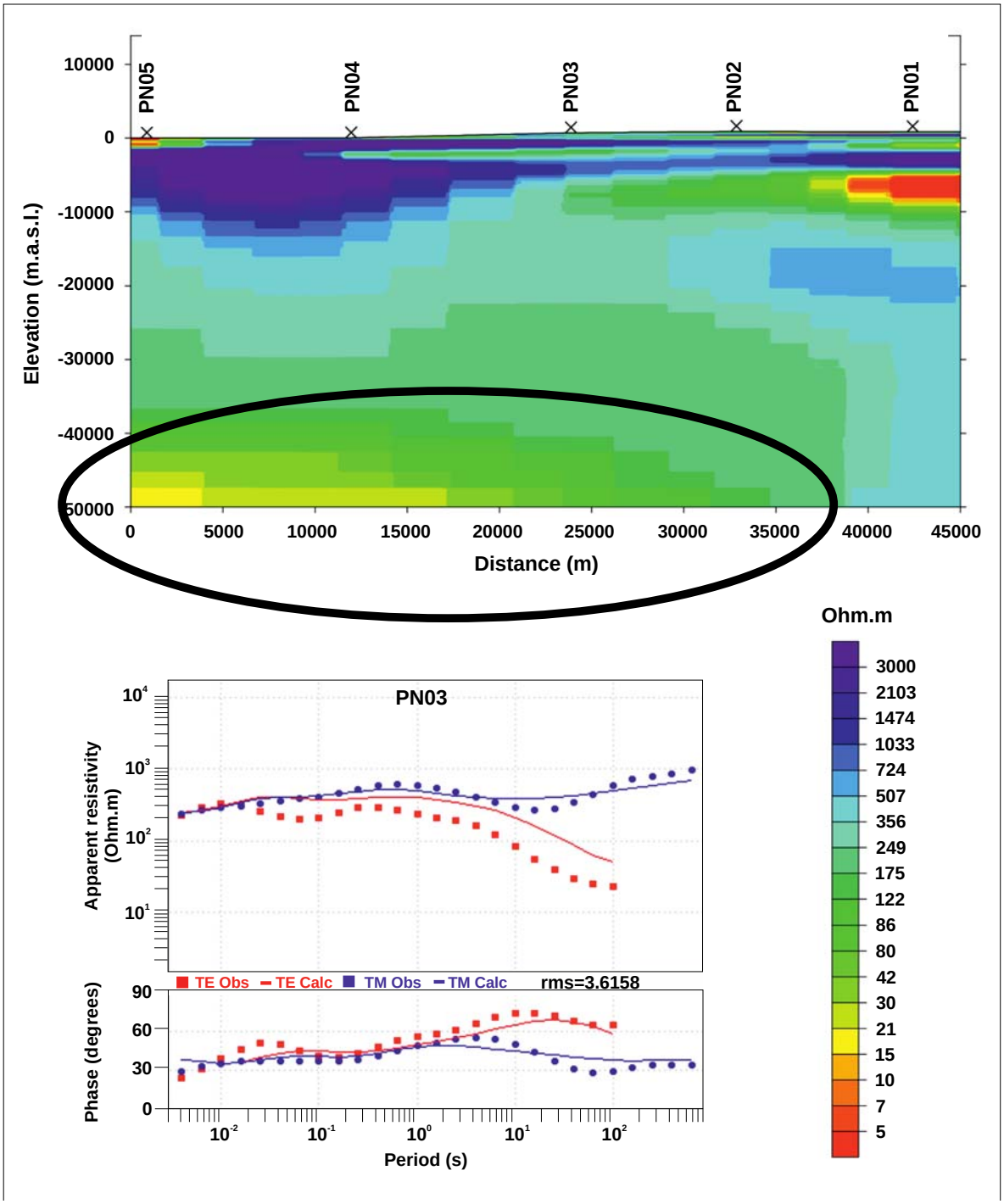

Figure DR9: The top figure shows the squeezing used in this case, which assumes that the top of the medium conductive body ranging from 30 to 122 Ohms (yellow-greenish colors), located to the middle of the profile is deeper. The bottom figure is explained in DR3, but uses PN03 instead of PN05.

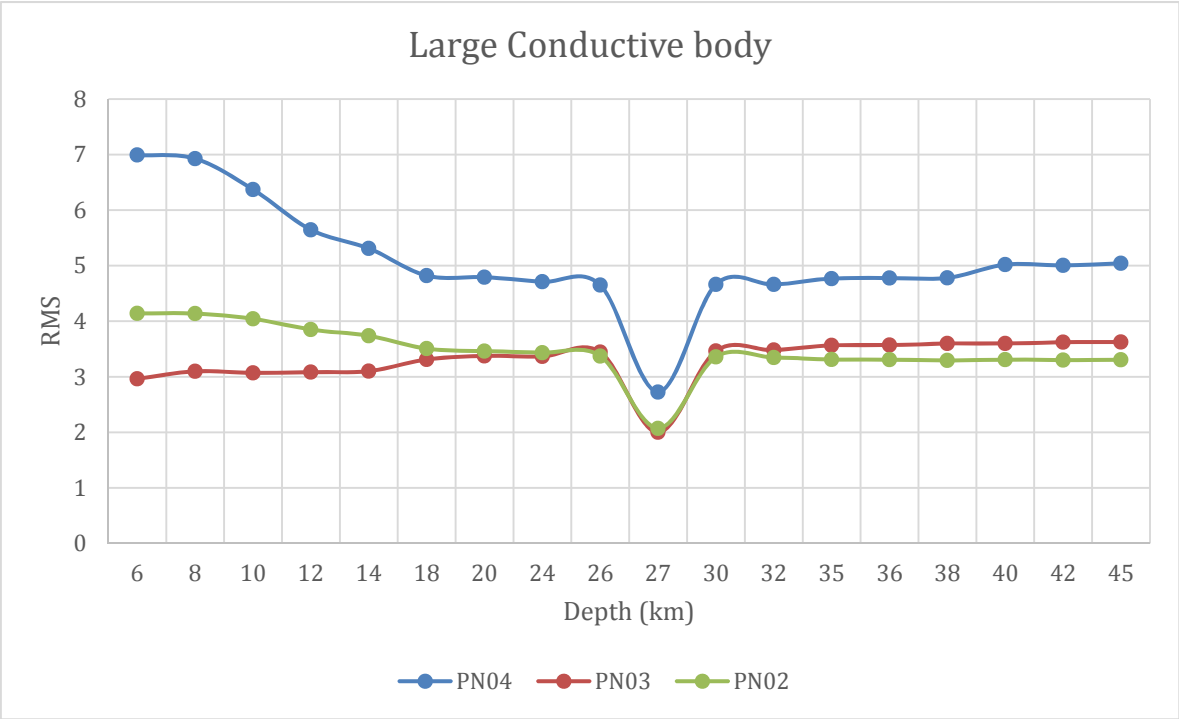

Figure DR10: This figure shows the RMS error from moving the conductive body in DR7 – DR9 steps of 2 km depths for stations PN04, PN03 and PN02 which are located above the body. They clearly show a strong minimum at the depth where our model finds the conductive body.

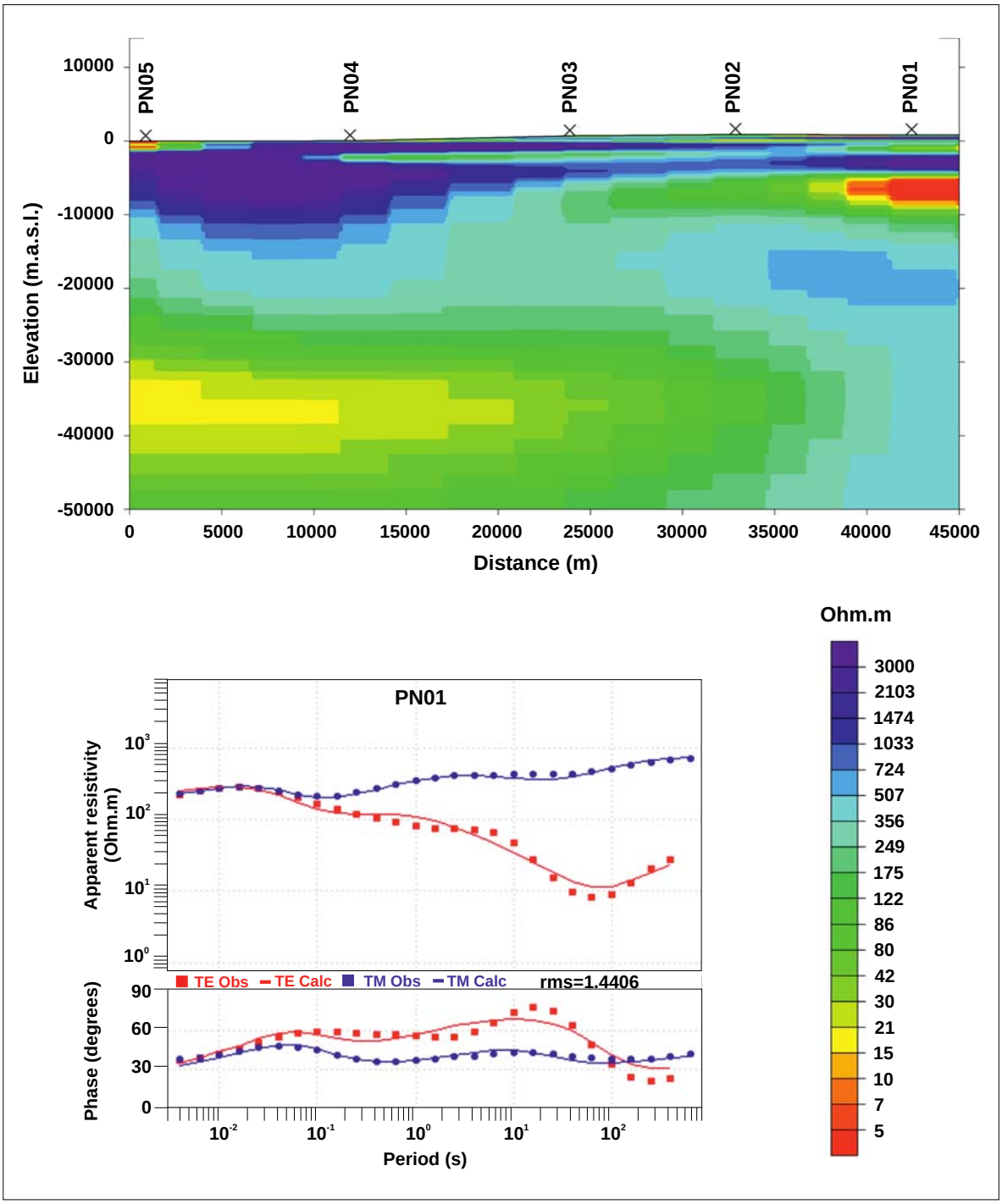

Figure DR11: The top figure shows the final model used in the main text. The bottom figure is explained in DR3, but is for sounding PN01 instead of PN05.

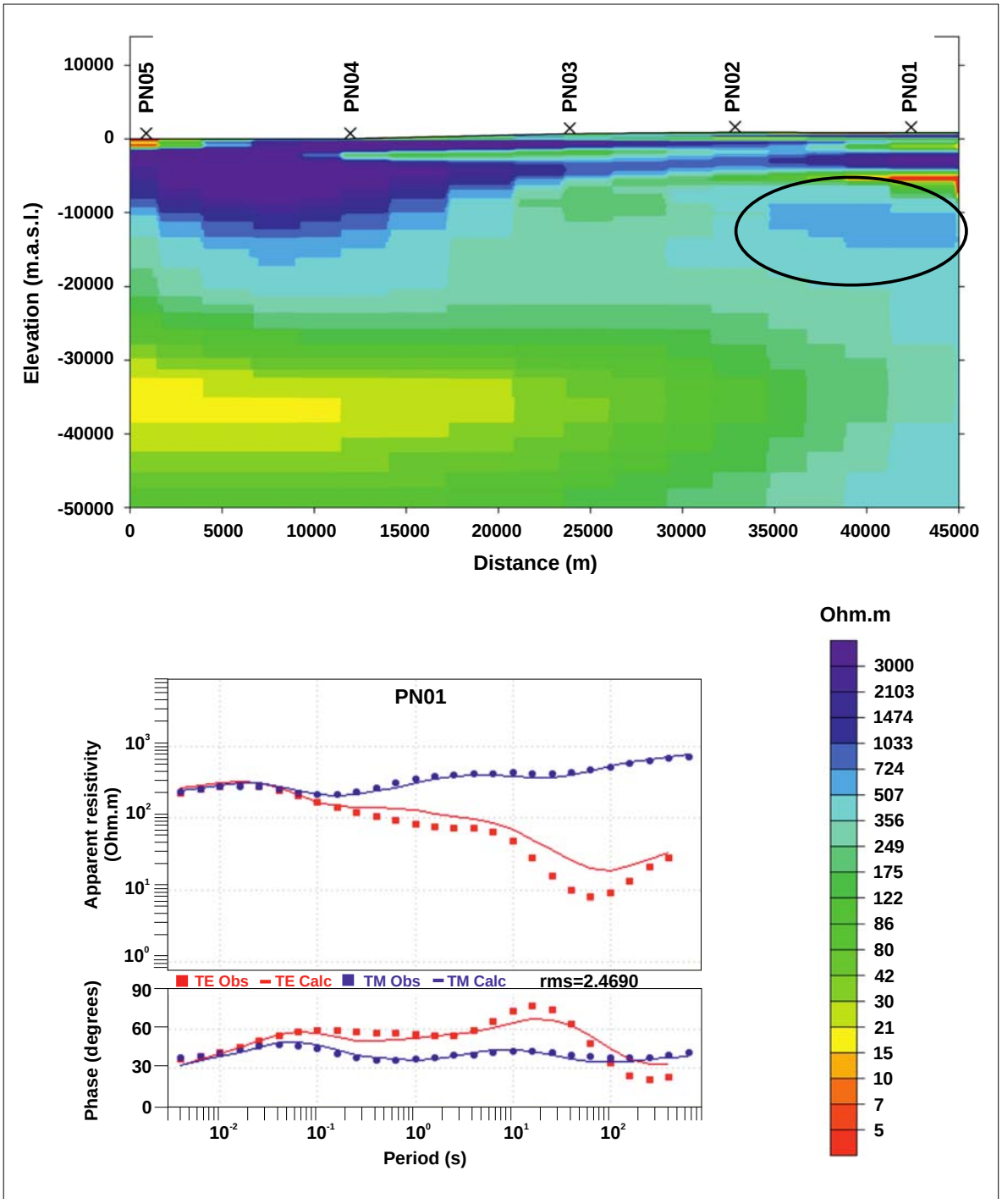

Figure DR12: The top figure shows the squeezing used in this case, which assumes that the top of the resistive body ranging from 500 to 700 Ohms (blue color), located to the northern sector of the profile is slightly shallower. The bottom figure is explained in DR3, but uses PN01 instead of PN05.

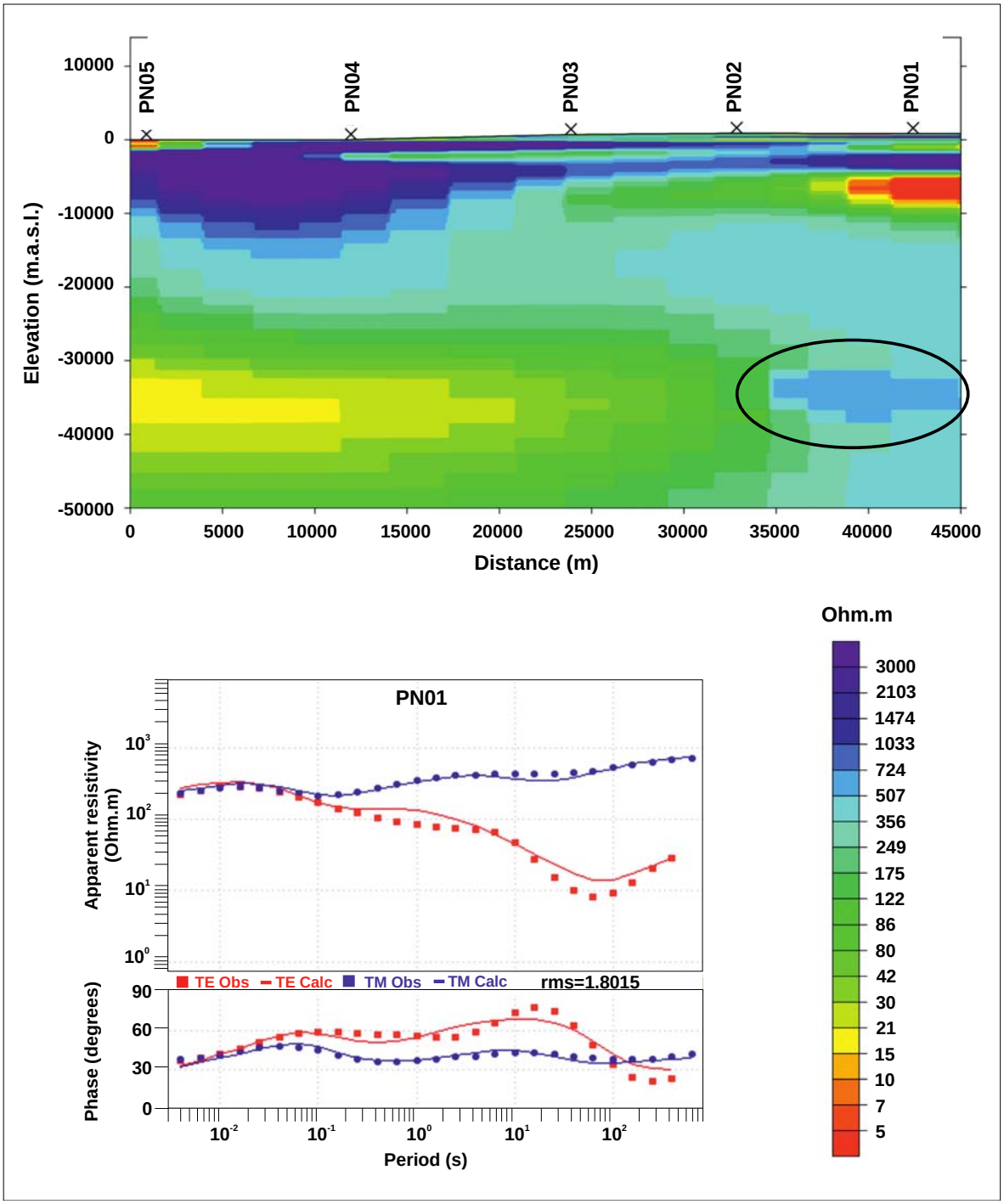

Figure DR13: The top figure shows the squeezing used in this case, which assumes that the top of the resistive body ranging from 500 to 700 Ohms (blue color), located to the northern sector of the profile is deeper. The bottom figure is explained in DR3, but uses PN01 instead of PN05.

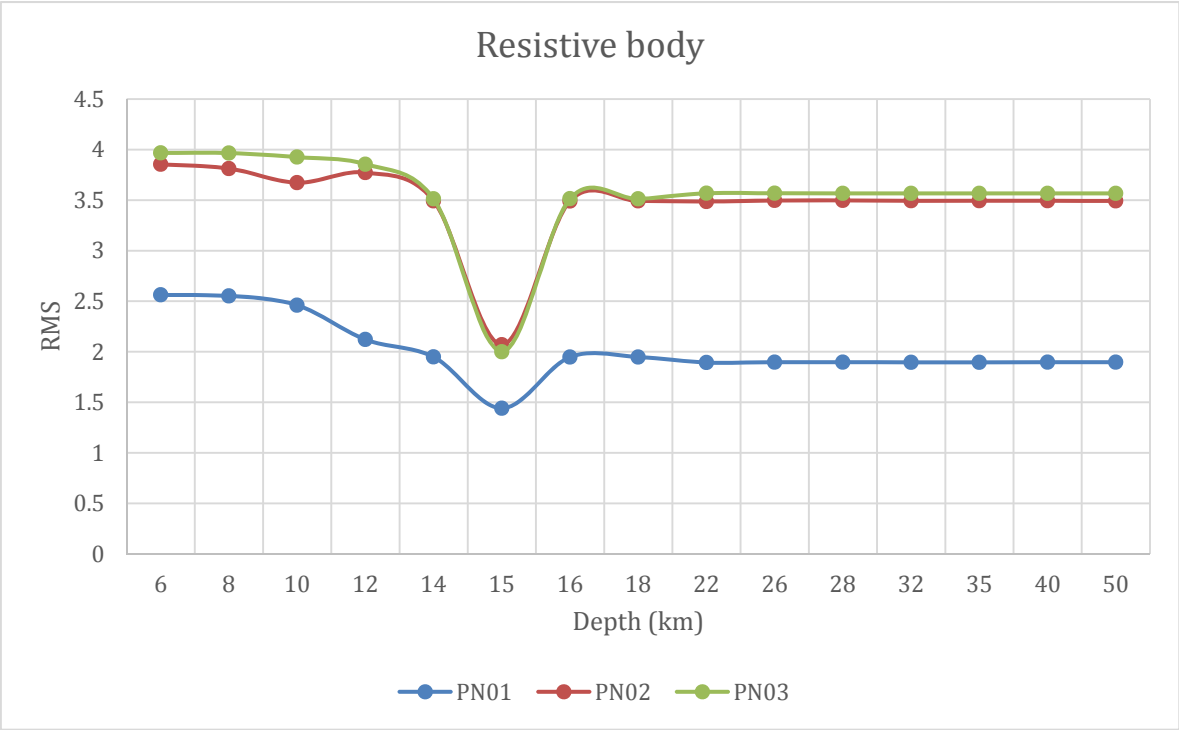

Figure DR14: This figure shows the RMS error from moving the conductive body in DR11 – DR13 steps of 2 km depths for stations PN01, PN02 and PN03 which are located above the body. They clearly show a strong minimum at the depth where our model finds the conductive body.

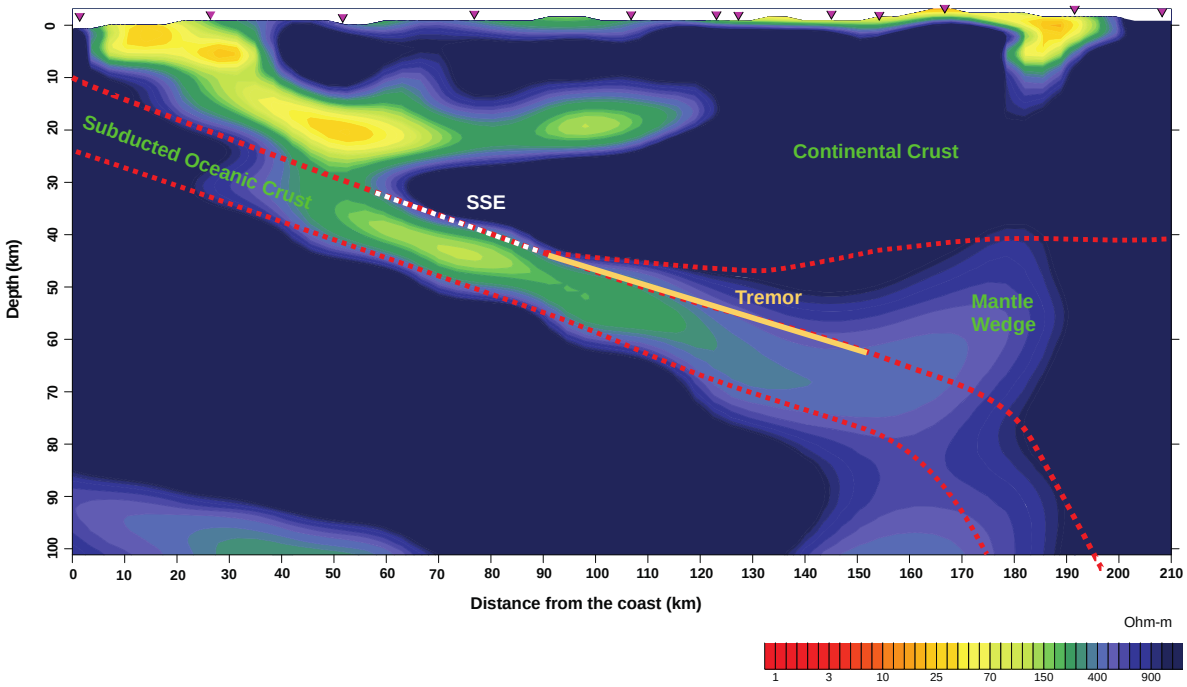

Figure DR15: The extended P4 MT inversion beyond the 50 km distance from the coast of the rest of the soundings. The soundings come from Arzate-Flores et al. (2016) and are reinterpreted here to have the same color scheme and impedance range as the rest of the soundings. The plate boundaries come from Arzate-Flores et al. (2016) with slight modifications from a seismic receiver function study that adds the corner of where the subducted plate plunges into the mantle (Rodríguez-Domínguez, 2016). The location of the SSE and the tremor comes from Brudzinski et al. (2010). The tremor is projected onto the plate interface since current understanding suggests that tremor lies on or near the interface and the actual depths in the study were poorly constrained (Brudzinski et al., 2010). The triangles are the locations of the soundings.

References not included in the main text

Allen, R.M., and Tromp, J., 2005. Resolution of regional seismic models: Squeezing the Iceland anomaly: Geophysical Journal International v. 161, p. 373–386, doi: 10.1111/j.1365-246X.2005.02600.x

Brudzinski, M., Prieto, H., Schlanser, K., Cano, E., Ceballos, A., Molina, O., and DeMets, C., 2010, Nonvolcanic tremor along the Oaxaca segment of the Middle America subduction zone: Journal of Geophysical Research: Solid Earth, v. 115, no. B8, doi: 10.1029/2008JB006061.

Corbo-Camargo, F., J. Arzate-Flores, R. Álvarez-Béjar, J. Aranda-Gomez, and V. Yutsis (2013), Subduction of the Rivera plate beneath the Jalisco block as imaged by magnetotelluric data, Revista Mexicana de Ciencias Geológicas, 30(2), 268–281.

Saltzer, R.L., and Humphreys, E.D., 1997. Upper mantle P wave velocity structure of the Eastern Snake River Plain and its relationship o geodynamic models of the region. Journal of Geophysical Research, v. 102, no. B6, p. 11,829-11,841.